Inorganic Chemistry

ARTICLE

pubs.acs.org/IC

Magnetic Ordering in Three-Dimensional Metal−Organic Frameworks Based on Carboxylate Bridged Square-Grid Layers

Qian Sun,[†] Ai-ling Cheng,[†] Yan-Qin Wang,[†] Yu Ma,[†] and En-Qing Gao*[,†]

[†]Shanghai Key Laboratory of Green Chemistry and Chemical Processes, Department of Chemistry, East China Normal University, Shanghai 200062, China

Supporting Information

ABSTRACT: Three isomorphous metal−organic frameworks of formula $[M(ppdc)(H_2O)_2]_n$ [M = Mn(II), Fe(II), and Co(II)] were synthesized from sodium *p*-phenylenediacrylic (Na_2ppdc). Crystallographic studies revealed that the compounds are layer-pillared 3D frameworks in which the square-grid M(II) layers with single carboxylate bridges are interlinked by long organic spacers with large interlayer separations of about 13 Å. Magnetic investigations indicated that they all display intralayer antiferromagnetic interactions through the carboxylate bridges in the unusual *skew−skew* coordination mode but the bulk behaviors are quite different. The Co(II) compound, like most compounds containing similar M−O−C−O−M layers, shows no 3D magnetic ordering down to 2 K, while the Mn(II) and Fe(II) compounds exhibit spin-canted ordering, behaving as a weak ferromagnet (T_C = 3.8 K) and a metamagnet (T_N = 3.8 K, H_c = 650 Oe), respectively. Spin-canted ordering is still a rarity in this series of materials. Magnetostructural comparisons with analogous compounds indicate that the occurrence of spin-canted ordering can be related to the uncommon *skew−skew* and *anti−anti* coordination modes of carboxylate bridges, which induce stronger antiferromagnetic interactions than the common *syn−anti* mode.

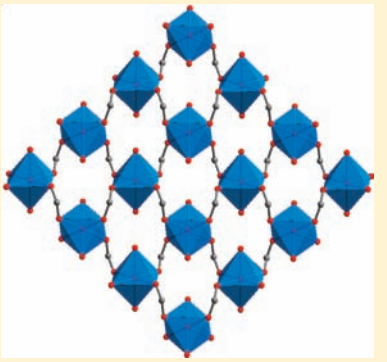

INTRODUCTION

The study of molecular magnetic materials has been of considerable interest for decades from both applied and fundamental points of view.[1,2] The great diversity and versatility in coordination and supramolecular chemistry have provided many low- and high-dimensional coordination systems that serve as models to understand the magnetostructural correlations, or as materials with useful magnetic properties. Metal−organic hybrid multilayer magnets, which consist of metal coordination layers and organic spacers, have attracted intense interest for several motivations: (i) to probe two-dimensional magnetism and its relevance to three-dimensional magnetism, (ii) to design molecular magnets with the properties controlled by the organic components, and (iii) to combine magnetism with other physical properties, taking advantage of the hybrid nature.[3] Carboxylate ligands have been widely used for designing magnetic systems for the versatility of the carboxylate group as a bridge to link two or more metal ions in various modes and to mediate magnetic exchanges of different nature.[4,5] Recently, the study has been much promoted by the exponential growth of metal−organic frameworks (MOFs) with di- or multicarboxylate ligands.[5] Many layered compounds with carboxylate ligands have M−O−M connections for layer formation (O arises from hydroxide or carboxylate), with or without M−O−C−O−M connections, and have been reported to behave as three-dimensionally ordered magnets.[5−12] For instance, $Co_2(OH)_2$(terephthalate) is a metamagnet with a high coercive field (>5 T at 1.5 K), among the hardest magnets.[6] The interlayer spacing can be chemically tuned by varying the dicarboxylate ligands, which does not affect the transition temperature but affects the metamagnetic transition field.[5,6] The simple M−O−C−O−M layer formed by only carboxylate bridges, exclusive of other intralayer covalent bridges, is also known,[4f,7,12−20] but three-dimensional (3D) ordering is rarely observed.[12−17] The structural factors determining whether or not the layers are magnetically ordered have yet to be clarified. Here we reported the synthesis, structure, and magnetic properties of a series of isomorphous multilayer compounds derived from *p*-phenylenediacrylic acid (H_2ppdc), for which the study of coordination chemistry is still limited.[21] The compounds, formulated as $[M(ppdc)(H_2O)_2]_n$ [M = Mn (**1**), Fe (**2**), and Co (**3**)], contain M−O−C−O−M square-grid layers with short intralayer bridges (the carboxylate groups) and long interlayer linkers (the organic backbone of the ligand), and they all exhibit intralayer antiferromagnetic (AF) coupling through carboxylate bridges, but the bulk magnetic behaviors are very different. While **3** shows no 3D magnetic ordering down to 2 K, **1** and **2** exhibit spin-canted ordering, behaving as a weak ferromagnet and a metamagnet, respectively. Magnetostructural comparisons with previous compounds containing similar layers are made to understand the different bulk behaviors.

EXPERIMENTAL SECTION

Materials and General Methods. All reagents were purchased from commercial sources and used without further purification.

Received: March 23, 2011
Published: August 05, 2011

p-Phenylenediacrylic acid (H_2ppdc) was prepared according to the literature.[22] Na_2ppdc was crystallized by adding ethanol to an aqueous solution of H_2ppdc and sodium hydroxide. Elemental analyses were determined on an Elementar Vario ELIII analyzer. The FT-IR spectra were recorded in the range 500−4000 cm^{-1} using KBr pellets on a Nicolet NEXUS 670 spectrophotometer. The phase purity of the samples was confirmed by powder X-ray diffraction collected on a Bruker D8-ADVANCE diffractometer equipped with Cu Kα at a scan speed of 1° min^{-1}. Magnetic measurements were carried out on a Quantum Design SQUID MPMS-5 magnetometer. Diamagnetic corrections were made with Pascal's constants.

Synthesis of Compounds 1−3. The compounds were synthesized by the liquid phase diffusion method. Above the aqueous solution (5 mL) of Na_2ppdc (0.10 mmol, 0.026 g) in a 25 mL clean tube, a mixture of ethanol and water in the volume ratio of 1:1 and an ethanol solution of $Mn(OAc)_2\cdot 4H_2O$ (0.1 mmol, 0.025 g) were successively addded dropwise to give a three-layer system, which was sealed and left undisturbed at room temperature. Slow diffusion yielded transparent and pale-amber lamellar crystals of **1** (0.018 g, 58% based on Mn) after 7 days. Anal. Found C 46.88, H 4.28. Calcd for $C_{12}H_{12}MnO_6$: C 46.92, H 3.94. IR (KBr, cm^{-1}): 3357br, 2926m 1645s, 1544s, 1392vs, 1260w, 983s, 890m, 835s, 696m, 511w. A similar procedure was followed to prepare **3** except that $Mn(OAc)_2\cdot 4H_2O$ was replaced by $Co(NO_3)_2\cdot 6H_2O$ (0.1 mmol, 0.03 g). Red block crystals in yield 45% (based on Co) were obtained. Anal. Found C 46.15, H 4.31. Calcd for $C_{12}H_{12}CoO_6$: C 46.32, H 3.89. IR (KBr, cm^{-1}): 3340br, 2920m, 1640vs, 1540s, 1390vs, 1255w, 984vs, 885w, 835m, 698m, 514w.

Crystals of **2** were grown by a similar diffusion method with some modification. A few drops of the ethanol solution of $Fe(ClO_4)_2\cdot 4H_2O$ was carefully added to the aqueous solution (5 mL) of Na_2ppdc (0.10 mmol, 0.026 g) in a clean tube. Khaki floc appeared at the interface immediately. A mixture of alcohol and water (5 mL, v/v = 1/1) was carefully added dropwise to form a buffer layer, and then an ethanol solution (5 mL) of $Fe(ClO_4)_2\cdot 4H_2O$ (0.035 g, 0.10 mmol) was dropped on the top. The tube was sealed and left undisturbed at room temperature. Orange block crystals of **2** appeared one week later, concomitant with some yellow amorphous precipitate. The crystals were collected by hand for characterization. Yield: 48% based on Fe. Anal. Found C 46.58, H 4.12. Calcd for $C_{12}H_{12}FeO_6$: C 46.79, H 3.93. IR (KBr, cm^{-1}): 3340br, 2920w, 1635s, 1544s, 1392vs, 1260w, 984s, 880w, 839m, 696m, 544w.

X-ray Crystallographic Measurements. Diffraction data were collected at ambient temperature on a Bruker Apex II CCD area detector equipped with graphite-monochromated Mo Kα radiation (λ = 0.71073 Å). Empirical absorption corrections were applied using the SADABS program.[23] The structures were solved by the direct method and refined by the full-matrix least-squares method on F^2, with all non-hydrogen atoms refined with anisotropic thermal parameters.[24] All the hydrogen atoms attached to carbon atoms were placed in calculated positions and refined using the riding model, and the water hydrogen atoms were located from the difference maps. All calculations were carried out with the SHELXTL crystallographic software. A summary of the crystallographic data and refinement parameters is provided in Table 1. CCDC 808155 (**1**), 808156 (**2**), and 808157 (**3**) contain the supplementary crystallographic data for this paper.

RESULTS AND DISCUSSION

Compounds **1**−**3** were synthesized as crystals from Na_2ppdc and appropriate metal salts by diffusion methods. The FT-IR spectra of compounds **1**−**3** are similar and show no absorption bands around 1700 cm^{-1}, consistent with the complete deprotonation of the carboxylic groups of the ppdc ligand in the compounds. The strong absorption in the range 1640−1645 cm^{-1} may be assigned to the υ_{as}(COO) vibration, and the strong bands at about 1390 cm^{-1} may be assigned to υ_s(COO). All the compounds show broad bands in the region 3300−3400 cm^{-1}, which can be assigned to water molecules.

Table 1. Crystal Data and Structure Refinement for Compounds 1−3

	1	2	3
formula	$C_{12}H_{12}MnO_6$	$C_{12}H_{12}FeO_6$	$C_{12}H_{12}CoO_6$
fw	307.16	308.07	311.15
crystal system	monoclinic	monoclinic	monoclinic
space group	$P2_1/c$	$P2_1/c$	$P2_1/c$
a/Å	13.088(5)	13.058(6)	12.903(7)
b/Å	6.461(2)	6.386(3)	6.371(3)
c/Å	7.461(3)	7.409(3)	7.329(4)
β/deg	91.175(5)	90.001(7)	90.289(7)
V/Å^3	630.9(4)	617.8(5)	602.4(5)
Z	2	2	2
D_c (g cm^{-3})	1.617	1.656	1.715
μ (mm^{-1})	1.065	1.240	1.444
F(000)	314	316	318
reflns collected	5124	3712	2737
unique reflns	1434	1280	1304
GOF on F^2	1.200	1.156	1.262
R_{int}	0.0321	0.0312	0.0418
R_1 ($I > 2\sigma(I)$)	0.0490	0.0726	0.0965
wR_2(all data)	0.1155	0.1862	0.2269

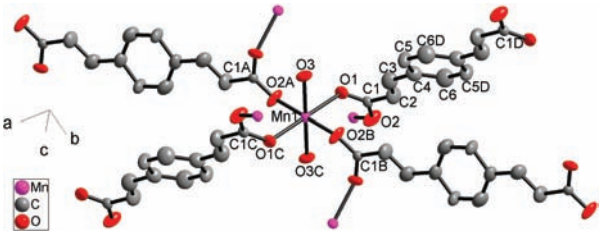

Figure 1. Coordination environment of Mn(II) in **1** with the ellipsoids drawn at the 50% probability level; hydrogen atoms are omitted for clarity.

Crystal Structures. Compounds **1**−**3** are isomorphous and exhibit three-dimensional structures in which M(II)-carboxylate layers are connected by the rigid ppdc ligands. The coordination sphere around each M(II) is centrosymmetric and consists of two oxygens from water molecules and four carboxylate oxygens from different ppdc ligands, with a *trans*-octahedral geometry, as exemplified by compound **1** in Figure 1, with selected distances and angles of the structures listed in Table 2. The bond distances decrease in the order Mn−O > Fe−O > Co−O, agreeing with the radius variation of the metal ions.

The carboxylate groups in the structures are all crystallographically equivalent, and each connects two M(II) ions related by the crystallographic 2_1 screw axis, with the M···M distances being 4.94, 4.89, and 4.86 Å for **1**−**3**, respectively. Consequently, each M(II) ion is linked to four neighbors through four carboxylate bridges to produce a (4,4) square grid layer along the *bc* plane (Figure 2a), in which all M(II) ions are coplanar and the carboxylate bridges are alternately below and above the plane of

dx.doi.org/10.1021/ic200592s |*Inorg. Chem.* 2011, 50, 8144–8152

Table 2. Selected Distances (Å) and Angles (deg) for Compounds 1−3[a]

	1 (M = Mn)	2 (M = Fe)	3 (M = Co)
M1−O1	2.178(3)	2.146(5)	2.116(6)
M1−O2A	2.134(3)	2.089(5)	2.044(6)
M1−O3	2.203(3)	2.133(5)	2.085(6)
O2B−M1−O1	94.51(12)	83.5(2)	94.8(3)
O2A−M1−O1	85.49(12)	85.6(2)	85.2(3)
O2B−M1−O3	84.21(11)	83.5(2)	85.4(3)
O1−M1−O3C	92.95(11)	93.21(19)	92.7(3)
O2A−M1−O3	95.79(11)	96.5(2)	94.6(3)
O1−M1−O3	87.05(11)	86.79(19)	87.7(3)
M1−O1−C1−O2	82.8(5)	90.1(7)	92.4(8)
M1−O2A−C1A−O1A	39.3(6)	30.7(8)	28.2(9)
M1···M1A	4.935(1)	4.891(1)	4.855(2)

[a] Symmetry operations: (A) $-x+1, y-{}^1/_2, -z+{}^1/_2$; (B) $x, -y+{}^1/_2, z+{}^1/_2$; (C) $-x+1, -y, -z+1$.

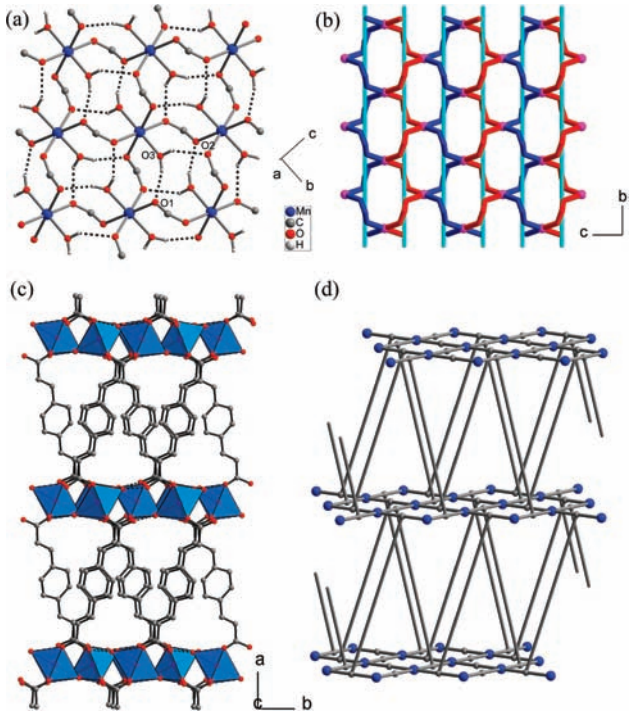

Figure 2. Views of the structure of **1**, showing (a) the $[M(OCO)_2]_n$ square-grid layer and the intralayer hydrogen bonds, (b) the alternation of $[M(OCO)]_n$ helical chains in the layer, (c) the layer-pillared 3D structure, and (d) the 3D net.

M(II) ions. The bridge adopts a highly nonplanar *skew−skew* coordination mode with the metal ions deviating much from the carboxylate plane on the opposite sides. This leads to a spiral conformation for the M−O−C−O−M moiety, with the M−O−C−O torsion angles being 82.8(5)° and 39.3(6)° for **1** (the parameters for **2** and **3** are included in Table 2). The bridging conformation leads to helical $[M(OCO)]_n$ chains along the *b* direction, and the 2D network can be regarded as consisting of left- and right-handed helical chains sharing the centrosymmetric M(II) sites. (Figure 2b). The helical feature dictates that neighboring metal coordination polyhedrons are inclined with

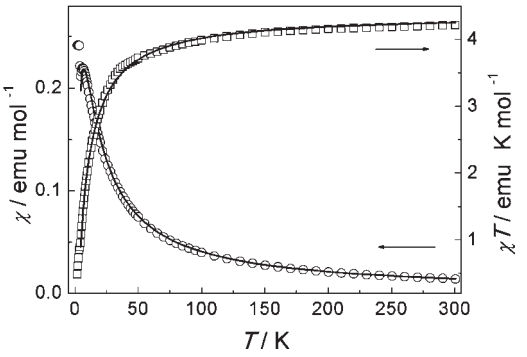

Figure 3. Magnetic susceptibility of **1** plotted as χ vs T and χT vs T curves with the best fit (solid lines) to Lines' expansion (see text).

respect to each other. The dihedral angles (δ) between the $[MO_4]$ equatorial planes defined by carboxylate oxygen atoms are 44.6°, 44.3°, and 45.9° for **1**−**3**, respectively, and the angles between neighboring O_{water}−M−O_{water} axes are 51.0°, 51.4°, and 51.3°, respectively. The coordination layer is further stabilized by intralayer hydrogen bonds: each coordinated water molecule (O3) around an M(II) ion donates its hydrogen atoms to two carboxylate oxygen atoms (O1 and O2) coordinated to different M(II) ions (Figure 2a). (The relevant parameters are listed in the Supporting Information.) The hydrogen bonds afford two independent O−H···O bridges between adjacent M(II) ions.

The ppdc ligands reside on inversion centers and serve as pillars interlinking the M(II) layers into a 3D coordination network (Figure 2c). The M···M distance separated by the long pillar is about 13 Å, corresponding to the *a* axes of the unit cells. Topologically, the 3D network results from the edge-to-edge connection of the (4,4) M(II)-carboxylate sheets; that is, the carboxylate edges of neighboring sheets are connected by the phenylenediethylene moieties. This is different from the usual node-to-node connection for most known layer-pillared networks.[25] It is convenient to regard the carboxylate groups as 3-connected nodes, with metal centers as 4-connected nodes, and then the 3D network can be reduced to a 3,4-connected net with a Schläfli symbol of $(8^3)_2(8^5 10)$, as illustrated in Figure 2d.

Magnetic Properties. Magnetically, all these compounds can be viewed as two-dimensional magnetic layers, in which each metal ion is coupled with four equivalent neighbors through single carboxylate bridges. The layers are separated far away by the backbone of ppdc, and hence, the interactions between layers can be neglected in a first approximation. Magnetic measurements of complexes **1**−**3** were performed on polycrystalline samples. The results are shown in Figures 3−10.

Mn(II) Complex ***1***. Figure 3 shows the thermal dependence of the magnetic susceptibility of compound **1** under an applied field of 1 kOe. As the temperature is lowered, the χT value decreases continuously, and the χ value first increases to a maximum at 6 K, then decreases slightly, and finally undergoes a rebound below 4.5 K. In the temperature region above 8 K, a typical paramagnetic Curie−Weiss behavior was observed, with the Curie and Weiss constants being $C = 4.27$ emu mol^{-1} K^{-1} and $\theta = -4.6$ K, respectively. The negative θ value and the decrease of the χT are indicative of AF interactions in the compound.

Treating the systems as AF square lattices, the susceptibility data have been analyzed by the following two approaches:

The first is the expansion series proposed by Lines[26] based on the exchange Hamiltonian $H = -\Sigma_{i,j} J S_i S_j$, where $\Sigma_{i,j}$ runs over all

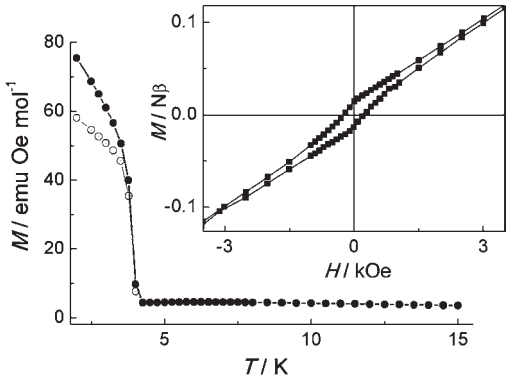

Figure 4. ZFC (open circles) and FC (filled circles) curves of **1** at 20 Oe. Inset: Hysteresis loop of **1** measured at 2 K.

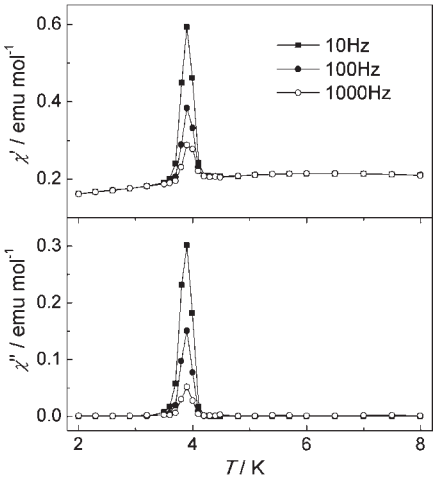

Figure 5. Temperature dependence of the ac magnetic susceptibility of compound **1** at zero dc field and different frequencies with a driving ac field of 3 Oe.

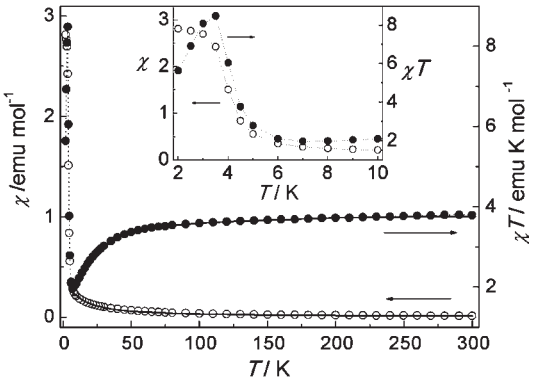

Figure 6. Magnetic susceptibility of **2** as χ and χT vs T plots with the best fit (solid lines) to Lines' expansion (see text). The dotted lines are a guide for the eye. The inset is a blow-up of the plots in the low temperature range.

pairs of nearest-neighbor spins i and j. The temperature dependence of the magnetic susceptibility is expressed as eq 1,

$$\chi = [Ng^2\beta^2/|J|]/[3\Theta + (\sum C_n/\Theta^{n-1})] \; (n = 1-6) \quad (1)$$

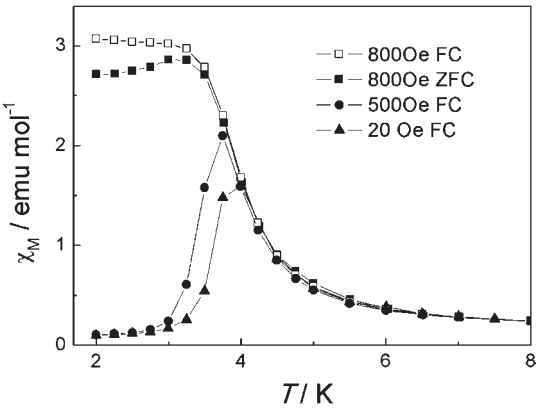

Figure 7. ZFC and FC $\chi(T)$ curves of **2** at different fields.

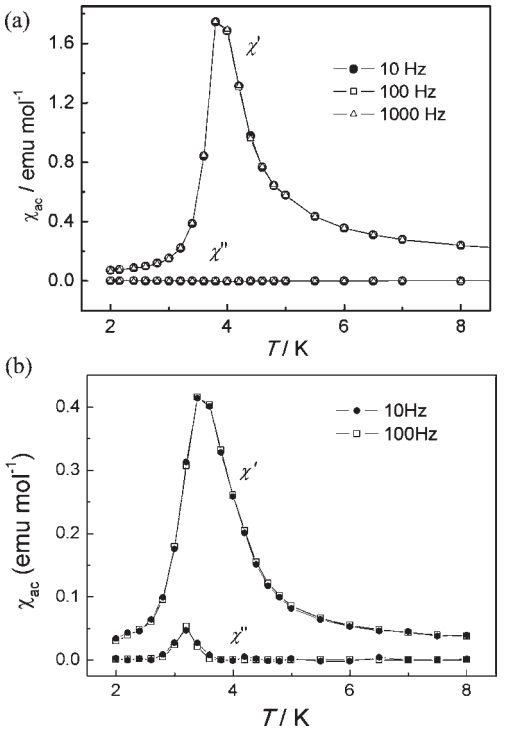

Figure 8. The ac magnetic susceptibility of compound **2** at different frequencies with a driving ac field of 3 Oe: (a) under zero static field and (b) under a 800 Oe static field.

in which $\Theta = kT/[|J|S(S+1)]$ with $S = {}^5/_2$. Nonlinear regression of the data of **1** above 4.5 K resulted in a best fit given by the parameters $J = -0.52$ cm^{-1} and $g = 2.00$.

The second approach uses the analytical expression [eq 2] derived by Curély for a square lattice of classical spins, based on the same Hamiltonian.[27]

$$\chi = [Ng^2\beta^2S(S+1)(1-u)^2]/[3kT(1-u)^2] \quad (2)$$

Here $S = {}^5/_2$ and u is the well-known Langevin function, $u = \coth[JS(S+1)/kT] - kT/JS(S+1)$. With g fixed at 2.00, the best fit above 4.5 K leads to $J = -0.45$ cm^{-1}. The J parameters obtained by the two approaches are very similar, and the small negative values corroborate the presence of weak AF interactions through the carboxylate bridges between Mn(II) ions.

dx.doi.org/10.1021/ic200592s |Inorg. Chem. 2011, 50, 8144–8152

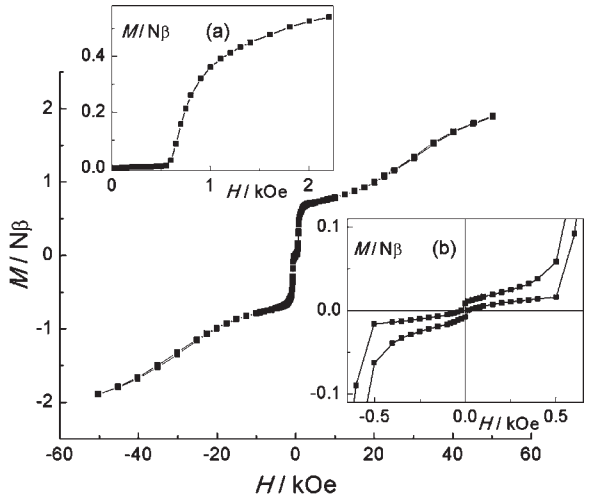

Figure 9. Isothermal magnetization of **2** measured by cycling the field between 50 and −50 KOe at 2 K. The insets show the low-field regions of the virgin magnetization curve (a) and hysteresis loop (b).

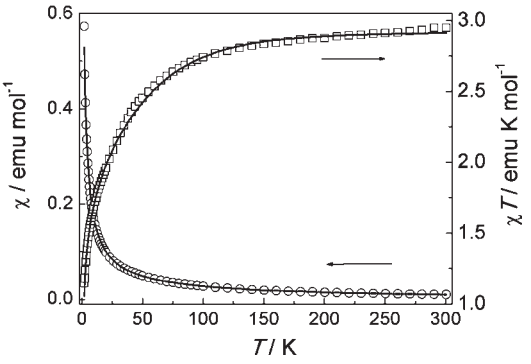

Figure 10. Magnetic susceptibility of **3** as χ and χT vs T plots with the best fit (solid lines) to the effective-spin approach (see text).

However, the intralayer AF interaction itself cannot account for the steep rise of χ below 4.5 K. To gain insight into the behavior, FC (field cooled) and ZFC (zero-field cooled) magnetization measurements under a field of 20 Oe were carried out. As shown in Figure 4, the FC magnetization begins to rise rapidly below 4.2 K and a divergence between the ZFC and FC curves occurs below 3.8 K, indicating the onset of weak ferromagnetic (FM) 3D long-range ordering below T_C = 3.8 K. The T_C value is confirmed by the observation that the $\partial\chi/\partial T$ derivative plots of the ZFC and FC data reach minimum values at 3.8 K. Isothermal magnetizations measured by cycling the field between ±50 kOe at 2 K revealed a small hysteresis loop with a remnant magnetization (M_r) of 0.014 Nβ and a coercive field (H_c) of 230 Oe (Figure 4 inset), confirming the occurrence of weak FM ordering. However, the magnetization value (2.08 Nβ) at 50 kOe is far below the saturation value (5 Nβ) expected for Mn(II) species, supporting the dominant AF coupling between Mn(II) ions. Alternating current magnetic measurements were performed at different frequencies under zero static field (Figure 5). The in-phase and out-of-phase components of the ac susceptibility both show maxima at a frequency-independent temperature (3.9 K), confirming the occurrence of the weak FM transition.

The above low-temperature behaviors are characteristic of weak ferromagnetism in spin-canted AF systems (sometimes called "canted antiferromagnetism" or "non-collinear antiferromagnetism"). Extrapolating the high-field linear region of the hysteresis loop to zero field gives a magnetization value of 0.019 Nβ, which may be taken as the magnetization contribution (M_w) from spin canting. Accordingly, the canting angle can be estimated to be $\alpha = 0.22°$ from the expression $\sin\alpha = M_w/M_S$, where M_S = 5 Nβ (the saturation magnetization for Mn(II)).

Fe(II) Complex **2**. The χ vs T and χT vs T plots measured under 1 kOe are reported in Figure 6. Upon cooling, χ increases gradually, then climbs rapidly, and finally approaches saturation at 2 K. The χT product decreases from 3.82 emu K mol^{-1} at room temperature down to a minimum of 1.98 emu K mol^{-1} at 7 K and then rises rapidly to a sharp maximum of 8.5 emu K mol^{-1} at 3.5 K. The $1/\chi$ vs T plot is linear above 100 K, following the Curie−Weiss law with the C and θ constants being 3.97 emu mol^{-1} K^{-1} and −11.6 K, respectively. The initial decrease of χT upon cooling and the negative Weiss constant indicate dominant AF interactions between Fe(II) ions, but the rapid rise in χT at low temperature is indicative of FM-like correlation. The magnetic properties are complicated by the presence of spin−orbital coupling and zero-field splitting intrinsic to the high-spin $^5T_{2g}$ ground state of octahedral Fe(II). For the lack of the appropriate 2D model combining the single-ion effects and the interion coupling, we are unable to evaluate the interaction parameter in **2**.

As observed for **1**, the low-temperature behaviors of **2** could be due to spin canting. To gain more information, FC and ZFC magnetization measurements were performed at different fields (Figure 7). The χT products at different fields all exhibit rapid rise below 7 K, suggesting that the AF layer has noncanceled magnetization due to the spin canting structure. At the field of 20 Oe, the ZFC and FC $\chi(T)$ curves coincide and reach a maximum at ca. 4 K, suggesting the occurrence of interlayer AF ordering (with "hidden" spin canting). The ordering is evoked by weak interlayer AF interactions, which cause an interlayer cancellation between the magnetizations of the spin-canted layers. At 500 Oe, the maxima shift to lower temperature. At 800 Oe, the ZFC and FC curves diverge, and the FC magnetization shows no maximum but approaches saturation below 4 K, indicating the onset of spontaneous magnetization. The behavior is indicative of field-induced metamagnetism, which means that the AF ordering between the spin-canted layers in **2** is broken by high field to generate a weak FM state. The metamagnetic behaviors are confirmed by the ac magnetic measurements (Figure 8). When measured in the absence of a static field (Figure 8a), the in-phase component (χ') of the magnetic susceptibility shows a frequency-independent maximum at T_N = 3.8 K, and no out-of-phase signal (χ'') was observed. The zero-field behavior is typical of antiferromagnets. When measured under a static field of 800 Oe (Figure 8b), the ac susceptibility shows frequency-independent nonzero χ'' signals maximized at 3.2 K, indicating that a weak FM state is induced by the static field. The phenomena are similar to those observed for a Co(II) multilayer metamagnet.[8]

The metamagnetic behavior is further confirmed by the sigmoidal shape of the magnetization vs field plot at 2 K (Figure 9, inset a): the magnetization first increases slowly with the field, as expected for typical antiferromagnets, and then increases abruptly above 500 Oe, indicating the field-induced transition from the AF (hidden spin canting) to a weak FM (spin canting) state. The critical field H_C is estimated to be about 650 Oe from

dx.doi.org/10.1021/ic200592s |*Inorg. Chem.* 2011, 50, 8144–8152

the $\partial M\ \partial H$ plot. The hysteresis loop at 2 K (Figure 9 and inset b therein) shows a small remnant magnetization of 0.009 Nβ and a coercive field of 200 Oe. The magnetization value (1.9 Nβ) at the highest field applied (50 kOe) is far below the saturation value M_S = 4.4 Nβ expected for Fe(II) species with $g \approx 2.2$, supporting the AF nature of the interactions between Fe(II) ions. Extrapolating the linear region from 2.5 to 8 kOe of the hysteresis loop to zero field gives M_w = 0.65 Nβ, from which the canting angle can be estimated to be $\alpha = 8.5°$.

Co(II) Complex **3**. The temperature dependences of χ and χT for compound **3** are shown in Figure 10. At room temperature, the χT values are near 3.00 emu K mol^{-1}, which is much larger than the spin-only value (1.88 emu K mol^{-1}) for $S = {}^3/_2$ but typical of octahedral Co(II) systems with a significant unquenched orbital momentum in the orbitally degenerate $^4T_{1\ g}$ ground state. As the temperature is lowered, χ and χT undergo continuous increase and decrease, respectively; no extreme values are observed down to 2 K. The thermal variation above 25 K follows the Curie−Weiss law with C = 3.11 emu mol^{-1} K and $\theta = -13.3$ K.

The decrease of χT upon cooling is due to the concurrent operation of the single-ion magnetic effect, intrinsic of pseudo-octahedral Co^{II} and the AF coupling between Co^{II} ions. The single-ion effect related to first-order spin−orbital coupling generates a Kramer's doublet ground state with an effective spin $S_{eff} = {}^1/_2$ for each Co(II). The depopulation of high-level states with decreasing temperature leads to a decrease in χT for an octahedral Co(II) system without interion magnetic coupling. Nevertheless, the presence of AF interactions between Co(II) ions is evidenced by the fact that the χT values (about 1.1 emu mol^{-1} K) for **3** at 2 K are significantly lower than the typical χT value of 1.5−2.0 emu mol^{-1} K for an isolated octahedral Co(II) system at very low temperature.[28,29]

To evaluate the interaction (J) between Co(II) ions, we employed the effective-spin approach proposed recently by Lloret et al.[29] In the framework of this approach, each Co(II) ion is treated as a $S_{eff} = {}^1/_2$ spin, which is related to the real spin ($S = {}^3/_2$) by $S = ({}^5/_3)S_{eff}$. The effective spin Hamiltonian for a square lattice can be expressed as follows:

$$\hat{\mathbf{H}} = -(25/9)J\sum_{i,j}\hat{\mathbf{S}}^i_{eff}\cdot\hat{\mathbf{S}}^j_{eff} - G(T,J)\beta H\sum_i \hat{\mathbf{S}}^i_{eff} \qquad (3)$$

where $G(T,J)$ is a fictitious and temperature-dependent Landé factor taking into account the influences of spin−orbital coupling, ligand-field distortion, and exchange coupling. An empirical expression of $G(T,J)$ has been derived,[29] and the variable parameters include λ (spin−orbital coupling parameter), α (orbital reduction factor), and Δ (ligand-field distortion factor, assuming an axial distortion), besides the magnetic exchange parameter (J). With this approach, the susceptibility of **3** can be expressed by a modified Lines' expansion for half-spin square lattices[26] (eq 1, with different C_n coefficients), where g is replaced by $G(T,J)$ and $\Theta = 12kT/(25|J|)$. The best-fit well reproduces the experimental data over the whole temperature range with $J = -0.23$ cm^{-1}, $\lambda = -105$ cm^{-1}, $\alpha = 1.38$, and $\Delta = 517$ cm^{-1}. The values of the single-ion parameters λ, α, and Δ lie in the usual ranges for octahedral Co(II), and the J value confirms the occurrence of weak AF coupling in **3**.

DISCUSSION

Among the numerous structures derived from transition metals and mono- or multicarboxylate ligands, those containing the rather simple square-grid layers based on M−O−C−O−M connections are relatively limited. With only a few exceptions with tetrahedral Co(II) coordination,[30] the layers contain octahedrally coordinated M(II) ions and have the general formula $[M(OCO)_2(X)_2]_n$. The layers can be either separated when monocarboxylate ligands are used[13,16,18,19] or interlinked into 3D frameworks by di-/tetra-carboxylate ligands[7,14,17,19,20] when X = O or N comes from solvents (mostly water) or α-hydroxyl/amine groups in some carboxylate ligands (e.g., tartrate and phenylglycinate).[31,32] Malonate as μ_3,η^4 chelating-bridging ligand has generated similar layers, for which, however, the carboxylate bridges are covalently connected within the layers.[33−35]

Magnetic studies on the Mn(II) species in the series have all indicated AF coupling through single carboxylate bridges,[18,31,36,37] consistent with our study on compound **1**. However, only a few of the species, [Mn(tartrate)] (T_C = 3.3 K)[31a] and [Mn(malonate)-$(H_2O)_2$] (T_C = 2.7 K)[34] in addition to the present compound **1** (T_C = 3.8 K), exhibit weak FM ordering above 2 K related to spin canting.[38] Spin canting behaviors have also been demonstrated in some other Mn(II) species with various bridges, although Mn(II) has very small g-factor anisotropy and weak zero-field splitting. Generally, spin canting can arise from two mechanisms:[39] (i) the antisymmetric Dzyaloshinsky−Moriya (DM) interaction; (ii) different anisotropy axes at neighboring metal sites. For both mechanisms, it is required that the relevant metal sites not be related by a center of symmetry. This is the case for the layer structures discussed here because the single carboxylate bridge is intrinsically incompatible with a symmetry center.

Then an interesting question arises: with similar layer structures without symmetry centers between neighboring metal sites, why do some compounds exhibit spin-canted ordering while some do not? The interlayer separation does not seem to be the critical factor, since the separations in the three ordered cases vary widely from 4.2 to 13.1 Å and lie within the range for the nonordered cases. As is well-known, the 3D ordering in multilayer systems can be evoked by (i) interlayer superexchange interactions, which propagate through bonds and vanish very rapidly as the distance increases, and/or (ii) interlayer dipolar interactions, which propagate through space and have long-range effects.[40] For 3D ordering dominated by interlayer dipolar interactions, Drillon and Panissod demonstrated that the ordering temperature is close to the temperature at which the intralayer correlation length reaches a threshold value, and hence, it depends only weakly upon interlayer spacing but mainly upon the divergence of the correlation length in the layer, which in turn depends upon the strength of intralayer interactions. The model has been applied to multilayer systems based on FM hydroxide layers[3a,40] and spin-canted azide layers.[41] It seems applicable to the present systems of carboxylate layers: the intralayer magnetic exchange in **1** ($J = -0.52$ cm^{-1}), [Mn(tartrate)] ($J = -0.40$ cm^{-1}),[31a] and [Mn(malonate)$(H_2O)_2$] ($J = -0.64$ cm^{-1})[34] is stronger than that ($J = -0.19$ to -0.30 cm^{-1}) in the Mn(II) compounds that do not exhibit spin-canted ordering above 2 K. The data seem to indicate that the occurrence of ordering is facilitated by stronger intralayer interactions.[40,41] It is assumed that the ordering temperature may be tuned by other factors, such as the nature of interchain connection, which may induce interlayer exchange, and the degree of spin canting, which influences the net moments of the layers. However, such correlations are not evident from the data of known compounds.

Furthermore, it seems that the magnitude of the intralayer interactions in this Mn(II) series can be correlated to the

coordination modes of carboxylate bridges. For most compounds in the series, the bridges adopt the usual *syn*−*anti* mode, which usually mediates weak exchange. Differently, half of the bridges in [Mn(malonate)$(H_2O)_2$][34] are in the *anti*−*anti* mode, and the bridge in **1** adopts the out-of-plane *skew*−*skew* mode. The single crystal structure of [Mn(tartrate)] is unavailable, but the bridge in the isomorphous Co analogue is intermediate between *syn*−*anti* and *skew*−*skew* (M−O−C−O, 157.9° and 30.4°).[31a] The *anti*−*anti* mode has been theoretically and experimentally demonstrated to be more efficient than the *syn*−*anti* mode in inducing AF interactions.[4a,42] Previous studies on the magnetic interaction through the *skew*−*skew* mode are still lacking, but the above magnetic and structural data indicate that it is also more efficient than *syn*−*anti*.

Fe(II)-carboxylate compounds are much less common than Co(II) and Mn(II) species in the literature, due to the synthetic difficulty arising from the sensitivity of Fe(II) to aerobic conditions. No Fe(II) structures containing the M−O−C−O−M square-grid layers have been characterized by single-crystal crystallography prior to this study. Only two previous compounds of this type, reported as the isomorphs of their Co(II) or Cu(II) analogues, have been synthesized from α-hydroxylcarboxylate ligands and magnetically studied.[31b] Both compounds show no indications of magnetic ordering down to 2 K. By contrast, compound **2** is a metamagnet (T_N = 3.8 K) exhibiting a field-induced transition (H_C = 650 Oe) from AF to weak FM ordering related to spin-canted AF layers. The magnetic difference of **2** from the previous two Fe(II) compounds is consistent with the magnetostructural correlations that we have just concluded for the Mn(II) species. A negligible magnetic interaction was reported for [Fe(mandelate)], in which the carboxylate bridge adopts the *syn*−*anti* mode according to the structural data for the isomorphous Cu(II) species.[31b] For [Fe(tartrate)], according to the crystallographic data for the isomorphous Co(II) species, the bridging mode is intermediate between *syn*−*anti* and *skew*−*skew*, which induces a weak AF interaction associated with a Weiss constant of θ = −5.8 K. Differently, the carboxylate bridge in **2** assumes the *skew*−*skew* mode. According to the conclusion we obtained for the Mn(II) series, the *skew*−*skew* mode induces stronger AF coupling than *syn*−*anti*. This is collaborated by the larger θ value of **2** (−9.1 K). Also as in the Mn(II) case, the stronger AF coupling favors the occurrence of long-range ordering in **2**. It is notable that the canting angle for **2** (8.5°) is significantly larger than that for **1** (0.22°), which may be a reflection of the fact that the Fe(II)-$^5T_{2g}$ ground state has significantly larger magnetic anisotropy than Mn(II)-$^6A_{1g}$.

Co(II) species with the M−O−C−O−M square-grid layers are relatively more common than Mn(II) and Fe(II).[6,15−20,31−33] However, the magnetic analysis is complicated by the intrinsic single-ion effects of octahedral Co(II). Some compounds were reported without quantitative magnetic analyses, and some were treated with oversimplified models without considering the single-ion effects. This situation makes it difficult to extract magnetostructural correlations. A survey suggests all the octahedral Co(II) compounds in this series do not exhibit long-range ordering above 2 K, except for [$Co(HCOO)_2(DMF)_2$],[15] which shows spin-canted ordering with T_C = 9 K. We noticed that the formate compound is also the only Co−O−C−O−Co layer compound with the bridge in the *anti*−*anti* mode. The unique magnetic and structural features of the formate compound collaborate the observation in the Mn(II) systems: the *anti*−*anti* mode induces a relatively strong AF interaction and hence tends to evoke ordering at relatively high temperature

To end the Discussion, we note that this series of compounds based on M(II)-carboxylate square-grid layers are in contrast with the $M^{II}_2(OH)_2$(terephthalate) series (M = Cu, Fe, Co), which are based on M(II)-hydroxide layers with auxiliary carboxylate bridges.[6,7,8b,12] While the Cu(II)-hydroxide layer exhibits intralayer FM interaction,[12] the Fe(II)- and Co(II)-hydroxide layers exhibit much stronger intralayer AF coupling than the M(II)-carboxylate layers. The $M^{II}_2(OH)_2$(terephthalate) series all exhibit long-range ordering, with the ordering temperatures being much higher than those for the present series. The quick comparisons seem to emphasize the importance of intralayer interactions in determining the ordering temperature, but the contributions from interlayer factors cannot be excluded. It is difficult to make detailed comparisons between the two series due to the wide differences in bridging networks.

CONCLUSION

In the present study, we have described three isomorphous metal−organic frameworks derived from *p*-phenylenediacrylic, in which the square-grid M(II) layers with single carboxylate bridges are pillared into 3D frameworks by long organic spacers with large interlayer separations of about 13 Å. They all display intralayer AF interactions through carboxylate bridges in the unusual *skew*−*skew* coordination mode, but the bulk behaviors are quite different. The magnetic properties have been compared with those of previous compounds containing similar M−O−C−O−M layers. The Co(II) compound (**3**), like most compounds in the series, shows no 3D magnetic ordering down to 2 K. Differently, compounds **1** is the third Mn(II) compound in the series that exhibits 3D ordering above 2 K, behaving as a weak ferromagnet due to spin canting, and compound **2** is the first 3D-ordered Fe(II) compound in the series, behaving as a metamagnet related to spin canting. Magnetostructural comparisons indicate that the occurrence of spin-canted ordering in **1** and **2** and the few previous compounds in the series can be related to the uncommon *skew*−*skew* and *anti*−*anti* coordination modes of the carboxylate bridges, which induce stronger AF interactions than the common *syn*−*anti* mode.

ASSOCIATED CONTENT

Supporting Information. Crystallographic data in CIF format and hydrogen bond distances and angles for all the crystal structures. This material is available free of charge via the Internet at http://pubs.acs.org.

AUTHOR INFORMATION

Corresponding Author

*E-mail: eqgao@chem.ecnu.edu.cn. Fax: (+86) 21-62233404.

ACKNOWLEDGMENT

This work is supported by the National Natural Science Foundation of China (NSFC) (91022017) and the Fundamental Research Funds for the Central Universities.

REFERENCES

(1) (a) Gatteschi, D.; Kahn, O.; Miller, J. S.; Palacio, F. *Magnetic Molecular Materials*; Kluwer Academic: Dordrecht, 1991. (b) Ito, K., Kinoshita, M., Eds.; *Molecular Magnetism: New Magnetic Materials*; Gordon and Breach: New York, 2000. (c) *Magnetism: Molecules to Materials*; Miller, J. S., Drillon, M., Eds.; Wiley-VCH: Weinheim, 2002−2005; Vols. I−V. (d) Special issue on Magnetism—Molecular, Supramolecular Perspectives. *Coord. Chem. Rev.* 2005, *249*. (e) Sun, H. L.; Wang, Z. M.; Gao, S. *Coord. Chem. Rev.* **2010**, *254*, 1081. (f) Murrie, M. *Chem. Soc. Rev.* **2010**, *39*, 1986. (g) Ishikawa, N. *Struct. Bonding (Berlin)* **2010**, *135*, 211. (h) Glaser, T. *Chem. Commun.* **2011**, *47*, 116.

(2) (a) Gonidec, M.; Luis, F.; Vilchez, A.; Esquena, J.; Amabilino, D. B.; Veciana, J. *Angew. Chem., Int. Ed.* **2010**, *49*, 1623. (b) Venkatakrishnan, T. S.; Sahoo, S.; Bréfuel, N.; Duhayon, C.; Paulsen, C.; Barra, A. L.; Ramasesha, S.; Sutter, J. P. *J. Am. Chem. Soc.* **2010**, *132*, 6047. (c) Miyasaka, H.; Takayama, K.; Saitoh, A.; Furukawa, S.; Yamashita, M.; Clérac, R. *Chem.—Eur. J.* **2010**, *16*, 3656. (d) Liu, T.; Zhang, Y. J.; Kanegawa, S.; Sato, O. *J. Am. Chem. Soc.* **2010**, *132*, 8250. (e) Jia, Q. X.; Tian, H.; Zhang, J. Y.; Gao, E. Q. *Chem.—Eur. J.* **2011**, *17*, 1040. (f) Guo, J.-F.; Wang, X.-T.; Wang, B.-W.; Xu, G.-C.; Gao, S.; Szeto, L.; Wong, W.-T.; Wong, W.-Y.; Lau, T.-C. *Chem.—Eur. J.* **2010**, *16*, 3524. (g) Hoshino, N.; Sekine, Y.; Nihei, M.; Oshio, H. *Chem. Commun.* **2010**, *46*, 6117.

(3) (a) Rabu, P.; Drillon, M.; Awaga, K.; Fujita, W.; Sekine, T. In *Magnetism: Molecules to Materials*; Miller, J. S., Drillon, M., Eds.; Wiley-VCH: Weinheim, Germany, 2001; pp 357−395. (b) Laget, V.; Hornick, C.; Rabu, P.; Drillon, M.; Ziessel, R. *Coord. Chem. Rev.* **1998**, *170−180*, 1533. (c) Rabu, P.; Drillon, M. *Adv. Eng. Mater.* **2003**, *5*, 189. (d) Delahaye, E.; Eyele-Mezui, S.; Diop, M.; Leuvrey, C.; Rabu, P.; Rogez, G. *Dalton Trans.* **2010**, *39*, 10577. (e) Kojima, N.; Okubo, M.; Shimizu, H.; Enomoto, M. *Coord. Chem. Rev.* **2007**, *251* (21−24), 2665.(f) Gòmez-Romero, P.; Sanchez, C. *Functional Hybrid Materials*; Wiley-VCH: 2004.

(4) (a) Rodríguez-Fortea, A.; Alemany, P.; Alvarez, S.; Ruiz, E. *Chem.—Eur. J.* **2001**, *7*, 627. (b) Zheng, Y. Z.; Tong, M. L.; Zhang, W. X.; Chen, X. M. *Angew. Chem., Int. Ed.* **2006**, *45*, 6310. (c) Nytko, E. A.; Helton, J. S.; Müller, P.; Nocera, D. G. *J. Am. Chem. Soc.* **2008**, *130*, 2922. (d) Caskey, S. R.; Wong-Foy, A. G.; Matzger, A. J. *J. Am. Chem. Soc.* **2008**, *130*, 10870. (e) Zhao, J. P.; Hu, B. W.; Lloret, F.; Tao, J.; Yang, Q.; Zhang, X. F.; Bu, X. H. *Inorg. Chem.* **2010**, *49*, 10390. (f) Li, Z. X.; Zhao, J. P.; Sañudo, E. C.; Ma, H.; Pan, Z. D.; Zeng, Y. F.; Bu, X. H. *Inorg. Chem.* **2009**, *48*, 11601.

(5) Kurmoo, M. *Chem. Soc. Rev.* **2009**, *38*, 1353and references therein.

(6) (a) Lovett, B. W.; Blundell, S. J.; Kumagai, H.; Kurmoo, M. *Synth. Met.* **2001**, *121*, 1814. (b) Huang, Z. L.; Drillon, M.; Masciocchi, N.; Sironi, A.; Zao, J. T.; Rabu, P.; Panissod, P. *Chem. Mater.* **2000**, *12*, 2805. (c) Rabu, P.; Huang, Z. L.; Hornick, C.; Drillon, M. *Synth. Met.* **2001**, *122*, 509. (d) Feyerherm, R.; Loose, A.; Rabu, P.; Drillon, M. *Solid State Sci.* **2003**, *5*, 321.

(7) Kurmoo, M.; Kumagai, H.; Green, M. A.; Lovett, B. W.; Blundell, S. J.; Ardavan, A.; Singleton, J. *J. Solid State Chem.* **2001**, *159*, 343.

(8) (a) Demessence, A.; Yassar, A.; Rogez, G.; Miozzo, L.; Brion, S. D.; Rabu, P. *J. Mater. Chem.* **2010**, *20*, 9401. (b) Mesbah, A.; Sibille, R.; Mazet, T.; Malaman, B.; Lebègue, S.; François, M. *J. Mater. Chem.* **2010**, *20*, 9386.

(9) (a) Zheng, Y. Z.; Tong, M. L.; Zhang, W. X.; Chen, X. M. *Chem. Commun.* **2006**, 165. (b) Kurmoo, M.; Kumagai, H.; Hughes, S. M.; Kepert, C. J. *Inorg. Chem.* **2003**, *42*, 6709.

(10) Rabu, P.; Rouba, S.; Laget, V.; Hornick, C.; Drillon, M. *Chem. Commun.* **1996**, *10*, 1107.

(11) Mesbah, A.; Carton, A.; Aranda, L.; Mazet, T.; Porcher, F.; Francois, M. *J. Solid State Chem.* **2008**, *181*, 3229.

(12) (a) Rabu, P.; Rueff, J. M.; Huang, Z. L.; Angelov, S.; Souletie, J.; Drillon, M. *Polyhedron* **2001**, *20*, 1677. (b) Abdelouhab, S.; François, M.; Elkaim, E.; Rabu, P. *Solid State Sci.* **2005**, *7*, 227.

(13) Beghidja, A.; Hallynck, S.; Welter, R.; Rabu, P. *Eur. J. Inorg. Chem.* **2005**, 662.

(14) Snejko, N.; Guttiérrez-Puebla, E.; Martínez, J. L.; Monge, M. A.; Ruiz-Valero, C. *Chem. Mater.* **2002**, *14*, 1879.

(15) Rettig, S. J.; Thompson, R. C.; Trotter, J.; Xia, S. *Inorg. Chem.* **1999**, *38*, 1360.

(16) Rueff, J. M.; Paulsen, C.; Souletie, J.; Drillon, M.; Rabu, P. *Solid State Sci.* **2005**, *7*, 431.

(17) Kumagai, H.; Kepert, C. J.; Kurmoo, M. *Inorg. Chem.* **2002**, *41*, 3410.

(18) Tangoulis, V.; Psomas, G.; Samara, C. D.; Raptopoulou, C. P.; Terzis, A.; Kessissoglou, D. P. *Inorg. Chem.* **1996**, *35*, 7655.

(19) Kumagai, H.; Oka, Y.; Inoue, K.; Kurmoo, M. *J. Chem. Soc., Dalton Trans.* **2002**, 3442.

(20) Fabelo, O.; Pasán, J.; Delgado, L. C.; Delgado, F. S.; Lloret, F.; Julve, M.; Pérez, C. R. *Inorg. Chem.* **2008**, *47*, 8053.

(21) (a) Fang, Q. R.; Zhu, G. S.; Xue, M.; Qiu, S. L. *Chem.—Eur. J.* **2006**, *12*, 3754. (b) Sun, Q.; Yue, Q.; Zhang, J. Y.; Wang, L.; Li, X.; Gao, E. Q. *Cryst. Growth Des.* **2009**, *9*, 2310.

(22) Fukuda, Y.; Seto, S.; Furuta, H.; Ebisu, H.; Oomori, Y.; Terashima, S. *J. Med. Chem.* **2001**, *44*, 1396.

(23) Sheldrick, G. M. *SADABS, Program for Empirical Absorption Correction*; University of Göttingen: Göttingen, Germany, 1996.

(24) Sheldrick, G. M. *SHELXTL*, Version 6.10; Bruker Analytical X-ray Instruments Inc.: Madison, WI, 1998.

(25) Hill, R. J.; Long, D. L.; Champness, N. R.; Hubberstey, P.; Schröder, M. *Acc. Chem. Res.* **2005**, *38*, 337.

(26) Lines, M. E. *J. Phys. Chem. Solids* **1970**, *31*, 101.

(27) (a) Curély, J. *Europhys. Lett.* **1995**, *32*, 529. (b) Curély, J. *Physica B* **1998**, *245*, 263. (c) Curély, J. *Physica B* **1998**, *254*, 277. (d) Curély, J.; Rouch, J. *Physica B* **1998**, *254*, 298.

(28) (a) Carlin, R. L. *Magnetochemistry*; Springer-Verlag: Berlin, Heidelberg, 1986. (b) Mabbs, F. E.; Machin, D. J. *Magnetism and Transition Metal Complexes*; Chapman and Hall, Ltd.: London, 1973. (c) Rueff, J. M.; Masciocchi, N.; Rabu, P.; Sironi, A.; Skaoulios, A. *Chem.—Eur. J.* **2002**, *8*, 1813. (d) Jankovics, H.; Daskalakis, M.; Raptopoulou, C. P.; Terzis, A.; Tangoulis, V.; Giapintzakis, J.; Kiss, T.; Salifoglou, A. *Inorg. Chem.* **2002**, *41*, 3366.

(29) Lloret, F.; Julve, M.; Cano, J.; Ruiz-García, R.; Pardo, E. *Inorg. Chim. Acta* **2008**, *361*, 3432.

(30) (a) Lee, E. W.; Kim, Y. J.; Jung, D. Y. *Inorg. Chem.* **2002**, *41*, 501. (b) Livage, C.; Egger, C.; Nogues, M.; Férey, G.; Acad., C. R. *Sci. Paris* **2001**, *4*, 221.

(31) (a) Coronado, E.; Galán-Mascarós, J. R.; Gómez-García, C. J.; Murcia-Martínez, A. *Chem.—Eur. J.* **2006**, *12*, 3484. (b) Beghidja, A.; Rogez, G.; Rabu, P.; Welter, R.; Drillon, M. *J. Mater. Chem.* **2006**, *16*, 2715.

(32) Duan, L. M.; Xie, F. T.; Chen, X. Y.; Chen, Y.; Lu, Y. K.; Cheng, P.; Xu, J. Q. *Cryst. Growth Des.* **2006**, 1101.

(33) Delgado, F. S.; Hernández-Molina, M.; Sanchiz, J.; Ruiz-Pérez, C.; Rodríguez-Martín, Y.; López, T.; Lloret, F.; Julve, M. *CrystEngComm* **2004**, *6*, 106.

(34) Martín, Y. R.; Molina, M. H.; Sanchiz, J.; Pérez, C. R.; Lloret, F.; Julve, M. *Dalton Trans.* **2003**, 2359.

(35) Manna, S. C.; Zangrando, E.; Drew, M. G. B.; Ribas, J.; Chaudhuri, N. R. *Eur. J. Inorg. Chem.* **2006**, 481.

(36) Konar, S.; Manna, S. C.; Zangrando, E.; Mallah, T.; Ribas, J.; Chaudhuri, N. R. *Eur. J. Inorg. Chem.* **2004**, 4202.

(37) Maji, T. K.; Sain, S.; Mostafa, G.; Lu, T. H.; Ribas, J.; Monfort, M.; Chaudhuri, N. R. *Inorg. Chem.* **2003**, *42*, 709.

(38) There is still a possibility that other compounds exhibit weak ferromagnetism at certain temperatures below 2 K (which is out of the usual temperature range measured), as demonstrated by the very-low-temperature study on a Mn(II) compound with phenoxyacetate, which has T_C = 1.63 K.Asaji, T.; Aoki, K.; Nakamura, D. *Z. Naturforsch.* **1984**, *39a*, 371.

(39) (a) Dzyaloshinsky, I. *J. Phys. Chem. Solids* **1958**, *4*, 241. (b) Moriya, T. *Phys. Rev.* **1960**, *120*, 91. (c) Moriya, T. *Phys. Rev.* **1960**, *117*, 635.

(40) (a) Panissod, P.; Drillon, M. In *Magnetism—From Molecules to Materials*; Miller, J. S., Drillon, M., Eds.; Wiley-VCH: Weinheim, 2002;

Vol. IV, pp 233−269. (b) Drillon, M.; Panissod, P. *J. Magn. Mater.* **1998**, *188*, 93.
(41) Gao, E. Q.; Liu, P. P.; Yue., Q.; Wang, Y. Q.; Wang, Q. L. *Chem.—Eur. J.* **2009**, *15*, 1217.
(42) Colacio, E.; Domínguez-Vera, J. M.; Ghazi, M.; Kivekäs, R.; Klinga, M.; Moreno, J. M. *Eur. J. Inorg. Chem.* **1999**, 441.